



# Pt nanoparticles entrapped in mesoporous metal–organic frameworks MIL-101 as an efficient catalyst for liquid-phase hydrogenation of benzaldehydes and nitrobenzenes

Huiyan Pan, Xiaohong Li\*, Yin Yu, Junrui Li, Jun Hu, Yejun Guan, Peng Wu

Shanghai Key Laboratory of Green Chemistry and Chemical Processes, Department of Chemistry, East China Normal University, 3663 North Zhongshan Rd., Shanghai 200062, China



## ARTICLE INFO

### Article history:

Received 4 December 2014

Received in revised form 13 January 2015

Accepted 18 January 2015

### Keywords:

Pt/MIL-101

Pt/Al<sub>2</sub>O<sub>3</sub>@SBA-15

Hydrogenation

Benzaldehyde

Nitrobenzene

Liquid-phase

## ABSTRACT

Metal organic-framework MIL-101 and inorganic mesoporous composites Al<sub>2</sub>O<sub>3</sub>@SBA-15 supported Pt catalysts, Pt/MIL-101 and Pt/Al<sub>2</sub>O<sub>3</sub>@SBA-15 catalysts, were prepared and characterized by means of X-ray diffraction (XRD), N<sub>2</sub> adsorption–desorption, scanning electron microscopy (SEM), transmission electron microscopy (TEM), CO chemisorption and thermo-gravimetric (TG) analysis. Pt nanoparticles were highly dispersed on both supports. In liquid-phase hydrogenation of nitrobenzene, benzaldehyde and their derivatives, the Pt/MIL-101 catalyst was superior to the Pt/Al<sub>2</sub>O<sub>3</sub>@SBA-15 catalyst in water. For liquid-phase hydrogenation of nitrobenzene with the Pt/MIL-101 catalyst, owing to high solubility of nitrobenzene in ethanol, the reaction in ethanol went much faster than that in water, furnishing a turnover frequency (TOF) in ethanol up to 18,053 h<sup>-1</sup>, almost triple of that obtained in water under similar conditions. The highest TOF of 25,438 h<sup>-1</sup> was obtained in ethanol for hydrogenation of 3-chloro-nitrobenzene with the Pt/MIL-101 catalyst. As for hydrogenation of benzaldehyde series, 2-fluoro-benzaldehyde and 3-fluoro-benzaldehyde gave the highest TOFs of 5146 h<sup>-1</sup> and 3165 h<sup>-1</sup> in water with the Pt/MIL-101 and Pt/Al<sub>2</sub>O<sub>3</sub>@SBA-15 catalysts, respectively. We deduce that surface property of MIL-101 with high hydrophobicity is helpful to enrich reactants around the Pt/MIL-101 catalyst in water, where nitrobenzene or benzaldehyde and its derivatives have a limited solubility, so that high catalytic performance was achieved with the Pt/MIL-101 catalyst in water. Of particular note is that the Pt/MIL-101 catalyst can be reused at least four times without loss in activity or selectivity.

© 2015 Elsevier B.V. All rights reserved.

## 1. Introduction

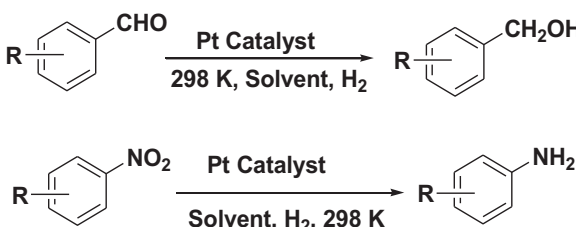
Hydrogenations of nitroarenes and aromatic aldehydes to corresponding aryl amines and aromatic alcohols are important processes in synthesis of dyes, pesticides, fine chemicals and pharmaceuticals. These transformations can be achieved either through hydrogen-transfer reduction [1–3] or by direct hydrogenation in heterogeneous system using atmospheric or compressed H<sub>2</sub> as hydrogen resource [4–8]. These heterogeneous hydrogenation processes are conducted usually in gas or liquid phase. Liquid phase hydrogenation systems have drawn much attention recently. Iron used to be a commonly applied catalyst in hydrogenation of nitroarenes [9–11], but was restricted due to relatively low catalytic ability and environmental pollution. With regard to heterogeneous liquid-phase catalytic hydrogenation of these compounds, Pt-based

catalysts are often used and supports are of varieties [6–8,12,13]. For instance, carbon materials supported Pt nanoparticles were active in hydrogenation of both benzaldehyde and nitrobenzene [7,12]. Especially for selective hydrogenation of nitrobenzene on Pt/MWCNTs (multi-walled carbon nanotubes), up to 66,900 h<sup>-1</sup> TOF was obtained [12]. Other supports, including mesoporous composites TiO<sub>2</sub>@SBA-15 [6] and metal–organic frameworks (MOFs) [8], were employed to immobilize Pt nanoparticles as efficient catalysts for the tested hydrogenation reaction.

In order to compare support effect on catalytic performance in liquid-phase hydrogenation of benzaldehydes and nitroarenes with supported Pt catalysts, herein, we chose two different mesoporous supports: the one is the MOFs and the other is an inorganic mesoporous composites. Recently, a great deal of attention has been attracted to design and application of MOFs because MOFs often possess large specific surface area and pore volume, porosity, well-defined structure, chemical tunability and flexibility and they can be used in different fields such as gas storage and separation, heterogeneous catalysis, molecular recognition and sensing,

\* Corresponding author. Tel.: +86 21 62238590; fax: +86 21 62238590.

E-mail address: [xhli@chem.ecnu.edu.cn](mailto:xhli@chem.ecnu.edu.cn) (X. Li).



and optics [14–18]. Due to high thermal stability, hydrothermal stability, acid–base resistance and mesoporous pores, MIL-101 MOFs, which were constructed by the link of terephthalic acid and the vertex of chromium oxo trime, have been extensively investigated in heterogeneous catalysis as catalyst alone [19–23] or as catalyst support [8,24–36]. For instance, Au nanoparticles, Pd nanoparticles, Pt nanoparticles and some bimetallic metals supported on MIL-101 exhibited good performances in hydrogenation [8,24–27], oxidation [28–31], decomposition [32–34] and other reactions [35,36]. In our previous work, Pt/MIL-101 catalyst was proved to be efficient and recyclable in asymmetric hydrogenation of  $\alpha$ -ketoesters after chirally modified with cinchona alkaloids and also showed comparable performance to commercial Pt/C and Pt/Al<sub>2</sub>O<sub>3</sub> catalysts [24].

The other concern is a kind of inorganic mesoporous composites, Al<sub>2</sub>O<sub>3</sub>@SBA-15, which was obtained by coating alumina inside mesoporous channels of SBA-15 through different methods. Al<sub>2</sub>O<sub>3</sub>@SBA-15 composites can not only take advantage of mesoporous materials SBA-15 with large specific surface area and uniform mesopore channel, but also exhibit properties not found in Al<sub>2</sub>O<sub>3</sub> alone. To be most important, Al<sub>2</sub>O<sub>3</sub>@SBA-15 supported Pt catalysts have been proved to be superior to pristine Al<sub>2</sub>O<sub>3</sub> supported one in enantioselective hydrogenation of  $\alpha$ -ketoesters after chirally modified with cinchona alkaloids as well [37,38].

Encouraged by these achievements, we were motivated to extend application of the Pt/MIL-101 and Pt/35AS (35AS denotes the Al<sub>2</sub>O<sub>3</sub>@SBA-15 composites where Al<sub>2</sub>O<sub>3</sub> loading is 35 wt.%) catalysts in liquid-phase hydrogenation of nitrobenzene and benzaldehyde and their derivatives (**Scheme 1**). Influences of support and solvent on catalytic performance were investigated. Mainly due to high hydrophobicity of MIL-101, the Pt/MIL-101 catalyst was more active than the Pt/35AS catalyst in water for the liquid-phase hydrogenation of nitrobenzene, benzaldehyde and their derivatives.

## 2. Experimental

### 2.1. Materials

Chloroplatinic acid hydrate (H<sub>2</sub>PtCl<sub>6</sub>·6H<sub>2</sub>O) (Pt ≥ 37%), terephthalic acid and chromium nitrate (Cr(NO<sub>3</sub>)<sub>3</sub>·9H<sub>2</sub>O) were purchased from Shanghai Experiment Reagent Co., Nitrobenzene and its derivatives were purchased from Aladdin and used as received. Benzaldehyde was of analytical grade and used as received and its derivatives were purchased from Alfa Aesar and used as received.

### 2.2. Catalyst preparation and characterization

#### 2.2.1. Catalyst preparation

MIL-101 was synthesized according to Ref. [19] with traditional hydrothermal method. Briefly, terephthalic acid (1.66 g, 10 mmol), Cr(NO<sub>3</sub>)<sub>3</sub>·9H<sub>2</sub>O (4.00 g, 10 mmol), 5 M aqueous HF (2 mL, 10 mmol) and deionized water (48 mL), were placed in a 200 mL Teflon-linear

autoclave and heated at 493 K for 8 h, and then further purified by twice solvothermal treatment in DMF (*N,N*-dimethylformamide) at 393 K for 8 h, and sequentially twice in ethanol at 353 K for 8 h. The resulting green powder was finally dried overnight at 373 K in oven for further use.

The 5 wt.% Pt/MIL-101 catalyst was prepared via a facile impregnation method [24]: MIL-101 was impregnated with an ethanolic solution containing H<sub>2</sub>PtCl<sub>6</sub> and stirred for 4–6 h. Then, the mixture was evaporated to remove excess solvent, followed by drying at 373 K overnight. The Pt precursor was reduced in an aqueous solution of sodium formate at 368 K for 2 h and then washed by plenty of water to remove chlorine anion. Finally, the sample was dried at 373 K overnight for further use. The 35AS was prepared using an ultrasonic impregnation method according to Ref. [38]. Procedure for preparing the 5 wt.% Pt/35AS catalyst was similar to that of the Pt/MIL-101 catalyst.

### 2.2.2. Catalyst characterization

XRD patterns of samples were collected on a Bruker D8 Advance instrument using Cu-K $\alpha$  radiation. The nitrogen adsorption–desorption isotherms were measured at 77 K on a Quantachrome Autosorb-3B system, after the samples were evacuated for 10 h at 473 K. The Brunauer–Emmett–Teller (BET) specific surface area was calculated using adsorption data in the relative pressure range from 0.05 to 0.35. The pore size distribution curves were calculated from the analysis of the adsorption branch of the isotherm using the Barrett–Joiner–Halenda (BJH) algorithm. The TEM images were taken on an FEI Tecnai G2-TF30 microscope at an acceleration voltage of 300 kV. The SEM images were taken on a Hitachi S4800 electron microscope with an acceleration voltage of 20 kV. The composition of samples was characterized by energy dispersive X-ray spectroscopy (EDX) using Horiba EMAX spectroscopy. The degree of dispersion and the mean particle size (cubic model) were estimated from the measured CO uptake, assuming a cross-sectional area for a surface platinum atom of  $8.0 \times 10^{-20} \text{ m}^2$  and a stoichiometric factor of one, using the nominal platinum concentrations. The TG analysis of the samples was conducted from ambient temperature to a required temperature under nitrogen atmosphere with Mettler Toledo TGA/SDTA851e apparatus. The Pt loading on samples was detected with a Thermo Elemental IRIS Intrepid II XSP inductively coupled plasma–atomic emission spectroscopy (ICP–AES).

### 2.3. Catalytic tests

For liquid-phase hydrogenation with the Pt/MIL-101 catalyst, 0.04 g or 0.05 g catalyst was pretreated under a hydrogen flow (40 mL/min) at 503 K for 2 h before use; while for the Pt/35AS catalyst involved hydrogenation, 0.05 g catalyst was used after pretreated under the similar conditions at 673 K for 2 h. The catalyst was then transferred to a 100 mL autoclave and mixed with solvent and substrate. The reaction began when hydrogen (4.0 MPa) was introduced with stirring at 298 K. The reaction was stopped after a proper time and products were analyzed by GC–FID (GC-2014, Shimadzu) equipped with a capillary column (DM-WAX, 30 m × 0.25 mm × 0.25  $\mu\text{m}$ ).

## 3. Results and discussion

### 3.1. Characterization of Pt catalysts

The MIL-101 support and the Pt/MIL-101 catalyst were characterized by XRD, N<sub>2</sub> sorption, SEM and TEM. The XRD pattern of Pt/MIL-101 catalyst demonstrates that the structure of the MIL-101 was well kept after Pt nanoparticles depositing (**Fig. 1a**). N<sub>2</sub> adsorption–desorption isotherms of MIL-101 and Pt/MIL-101 are

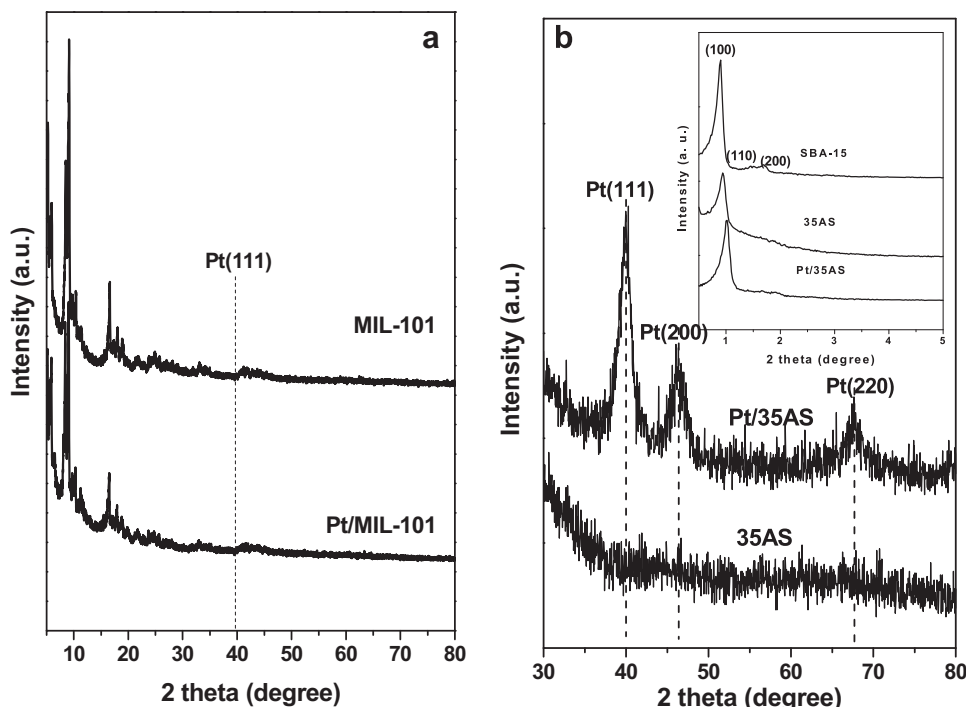


**Fig. 1.** XRD patterns of (a) MIL-101 and Pt/MIL-101; (b) 35AS and Pt/35AS.

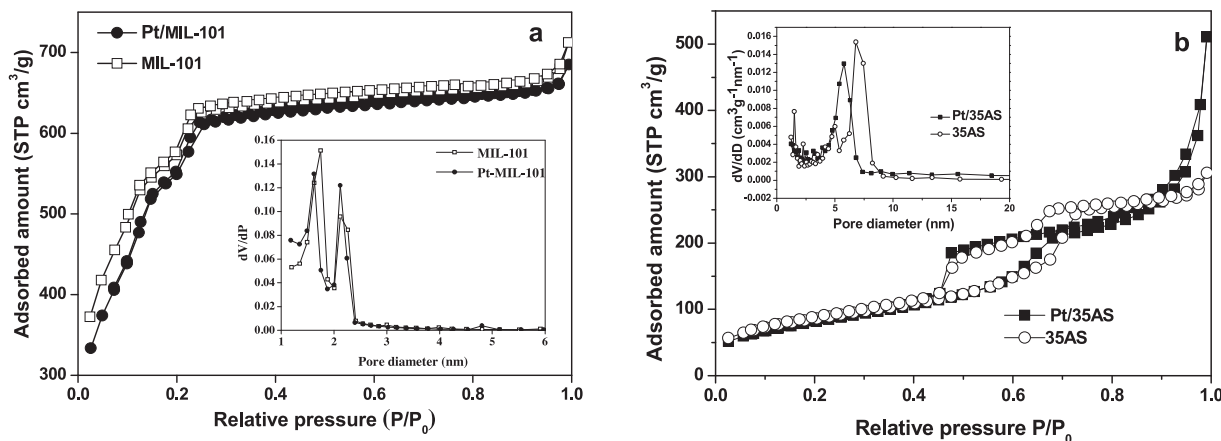
almost same (Fig. 2a). There are no obvious changes in BET specific surface areas (above 2000 m<sup>2</sup>/g) and pore size distribution after Pt nanoparticles deposited on MIL-101. SEM images in Fig. 3a and b show that morphology of MIL-101 and Pt/MIL-101 crystals is nearly same and both of them are homogeneously dispersed with irregular shapes. The distribution of Pt nanoparticles was characterized by TEM firstly. As displayed in Fig. 4a, the Pt nanoparticles are highly dispersed on the MIL-101. The dispersion of Pt nanoparticles was also measured by CO chemisorption and average Pt particle size is 2.9 nm with a dispersion of 37.9%.

Similarly, the 35AS composites and the Pt/35AS catalyst were also characterized using these techniques. The Pt/35AS catalyst reserves structure of 35AS composites (Fig. 1b) and BET specific surface area is decreased from 307 to 296 m<sup>2</sup>/g after Pt nanoparticles deposition (Fig. 2b). Moreover, morphology of catalyst is almost as same as that of 35AS composites (Fig. 3c and d). TEM image in Fig. 4b illustrates that Pt nanoparticles are highly dispersed on support and calculated results according to CO chemisorption give an

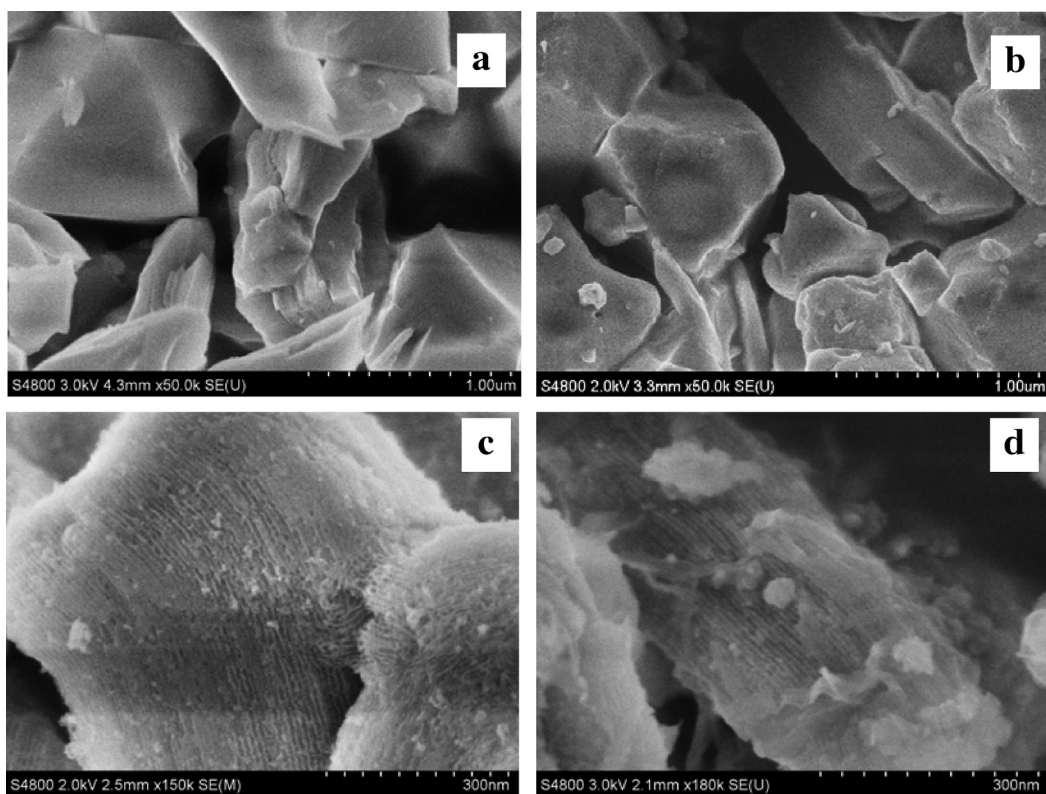
average Pt particle size of 2.4 nm with a dispersion of 45.8%. The detailed physicochemical parameters for these two catalysts are also listed in Table 1 for clarity.

### 3.2. Hydrogenation of nitrobenzene and its derivatives

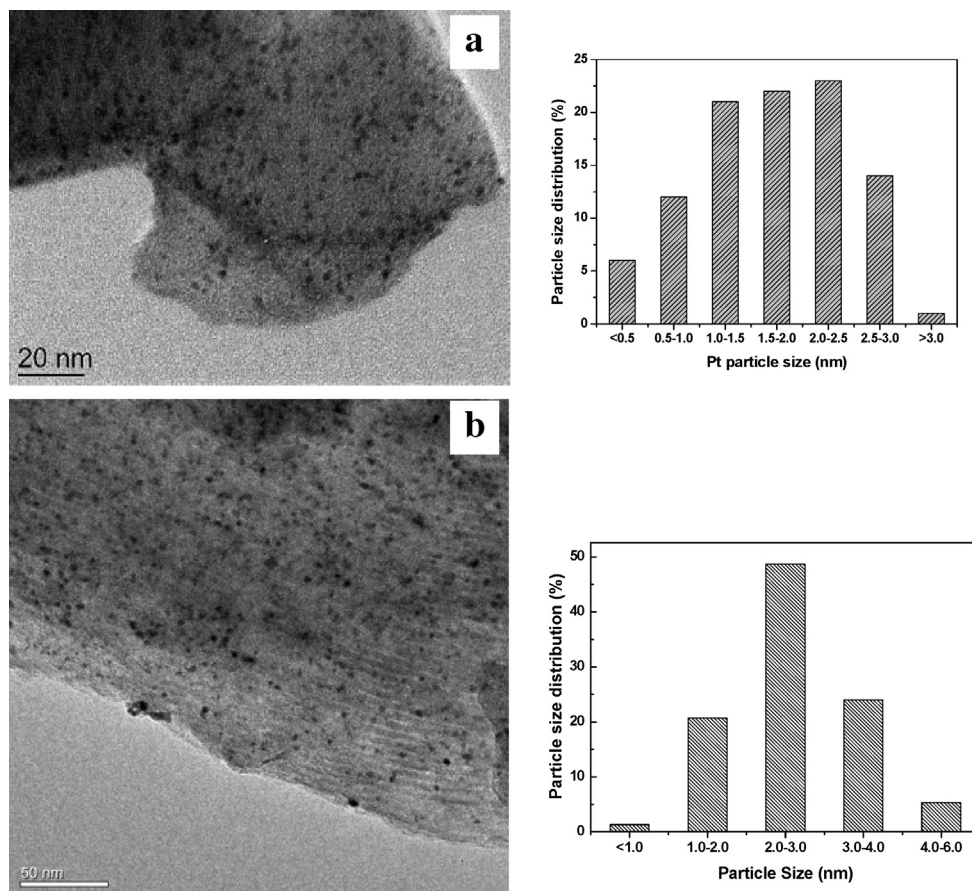
In order to investigate catalytic performance of Pt catalysts supported on different materials in liquid-phase hydrogenation of nitrobenzene and its derivatives, kinetic profile for hydrogenation of nitrobenzene with the Pt/MIL-101 catalyst in water was tested firstly. As shown in Fig. 5, conversion of nitrobenzene increased with reaction time almost linearly. About 32.5% conversion was obtained within 15 min and 62.9% of nitrobenzene was converted to aniline after 30 min. The reaction nearly completed after 45 min with 96.1% conversion, affording a TOF of 6673 h<sup>-1</sup>. The reaction rate did not change with proceeding of nitrobenzene reduction, so that we deduce that the hydrogenation of nitrobenzene with the Pt/MIL-101 catalyst was an apparent zero-order reaction. Besides



**Fig. 2.** N<sub>2</sub> sorption isotherms and pore size distributions (inset) of (a) MIL-101 and Pt/MIL-101 catalyst; (b) 35AS and Pt/35AS catalyst.



**Fig. 3.** SEM images of (a) MIL-101, (b) Pt/MIL-101, (c) 35AS and (d) Pt/35AS.

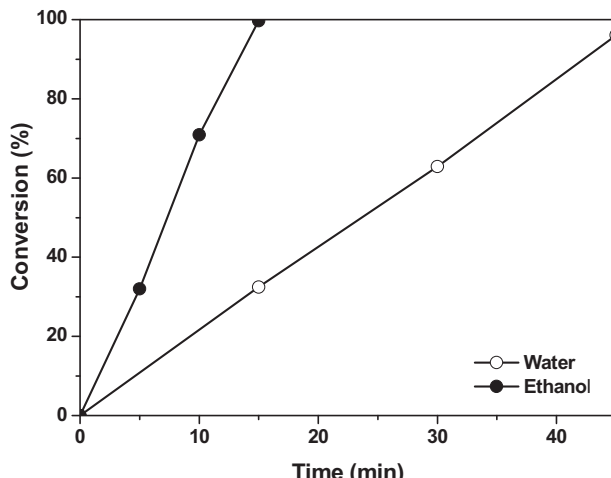


**Fig. 4.** TEM images of (a) Pt/MIL-101 catalyst and (b) Pt/35AS catalyst and their particle size distributions.

**Table 1**

The relevant physicochemical parameters for supports and catalysts

Entry	Sample	$S_{\text{BET}}^{\text{a}}$	$D_p^{\text{a}}$	Pt size	Pt particle	Pt loading (wt.%)	
		( $\text{m}^2 \text{ g}^{-1}$ )	(nm)	b(nm)	disp. (%)	EDX	ICP
1	MIL-101	2295	1.6, 2.1	—	—	—	—
2	Pt/MIL-101	2217	1.6, 2.1	2.9	37.9	4.6	4.9
3	35AS	307	6.8	—	—	—	—
4	Pt/35AS	296	5.8	2.4	45.8	3.5	3.7

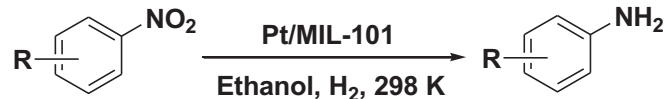
<sup>a</sup> Determined by  $\text{N}_2$  adsorption.<sup>b</sup> Average Pt particle size was determined by CO chemisorption.**Fig. 5.** Kinetic profiles of hydrogenation of nitrobenzene in different solvents with the Pt/MIL-101 catalyst. Reaction conditions: 21 mmol nitrobenzene, 4 MPa  $\text{H}_2$ , 298 K, 0.04 g Pt/MIL-101 for the reaction in 20 mL water or 0.05 g Pt/MIL-101 for the reaction in 20 mL ethanol.

in water, we also conducted the reaction in ethanol for comparison. To our delight, the hydrogenation of nitrobenzene with the Pt/MIL-101 catalyst went much faster in ethanol. It afforded 32.3% conversion within 5 min, 70.9% conversion in 10 min and nearly full conversion within 15 min. The highest TOF reached  $18,053 \text{ h}^{-1}$  with the Pt/MIL-101 catalyst in ethanol. The rate in ethanol was almost triple of that in water. The reason that nitrobenzene hydrogenation went faster in ethanol than in water could be explained in terms of higher solubility of nitrobenzene in ethanol, giving rise to a higher diffusion rate of nitrobenzene in ethanol.

For comparison, we also carried out the liquid-phase hydrogenation of nitrobenzene with the Pt/35AS catalyst. Under the same conditions, the hydrogenation of nitrobenzene with the Pt/35AS catalyst in water went quite slowly, only obtaining a conversion of 75% within 1 h, affording a TOF of  $3626 \text{ h}^{-1}$ , which was about half of that obtained with the Pt/MIL-101 catalyst.

Based on the results discussed above, we found that using the Pt/MIL-101 catalyst and using ethanol as solvent are a better choice for hydrogenation of nitrobenzene. Therefore, we adopted the Pt/MIL-101 catalyst to extend hydrogenation of nitrobenzene derivatives in ethanol.

To understand an effect of substituent group at aromatic ring, the hydrogenation of nitrobenzenes with different substituents at phenyl ring was carried out with the Pt/MIL-101 catalyst in ethanol. Due to high reactivity of the Pt/MIL-101 catalyst in ethanol, the hydrogenation of nitrobenzene derivatives in ethanol was stopped after 10 min. Table 2 lists the detailed results obtained for the hydrogenation of nitrobenzene derivatives with different substituents at the phenyl ring with the Pt/MIL-101 catalyst. For an electron-withdrawing substituent such as Cl<sup>-</sup> group, the *meta*- and *para*-substituted chloronitrobenzene were

**Table 2**  
Hydrogenation of nitrobenzenes with the Pt/MIL-101 catalyst in ethanol

Entry	R-group	Conv. (%) <sup>a</sup>	Sel. (%)	TOF ( $\text{h}^{-1}$ ) <sup>b</sup>
1	4-Cl	99.8	77.3	25,412
2	3-Cl	99.9	96.7	25,438
3	2-Cl	5.5	94.8	1,400
4	2-CH <sub>3</sub>	21.5	>99.0	5,474
5	3-CH <sub>3</sub>	97.6	>99.0	25,036
6	4-CH <sub>3</sub>	62.7	>99.0	15,965
7	2-CH <sub>3</sub> O	0.3	>99.0	77
8	4-CH <sub>3</sub> O	5.8	>99.0	1,477

Reaction conditions: 21 mmol nitroarenes, 4 MPa  $\text{H}_2$ , 298 K, 0.05 g Pt/MIL-101 catalyst (0.06 mol% Pt), 20 mL ethanol, 10 min.

<sup>a</sup> Conversion was based on GC-FID.<sup>b</sup> The TOF was calculated as converted substrate per mol of exposed Pt atoms per hour according to Pt loading detected by ICP-AES.

almost fully hydrogenated within 10 min, although selectivities to their target products were slightly lower, affording 96.7% and 77.3%, respectively (Table 2, entries 1 and 2). On the contrary, their *ortho*-substituted isomer only gave a 5.5% conversion with selectivity of 94.8% to 2-chloro-aniline (Table 2, entry 3). For an electron-donating substituent, such as methyl group substituted nitrobenzenes, the hydrogenation of the *ortho*-substituted nitrobenzene obtained 21.5% conversion (Table 2, entry 4); lower than those obtained with its *meta*- and *para*-isomers. As a result, 3-methyl-nitrobenzene and 4-methyl-nitrobenzene showed 97.6% and 62.7% conversions, respectively (Table 2, entries 5 and 6). For methoxy substituted nitrobenzene derivatives, both 2-methoxyl-nitrobenzene and 4-methoxyl-nitrobenzene were inactive under the tested conditions, only giving 0.3–5.8% conversions (Table 2, entries 7 and 8). These results showed that in ethanol, whatever the electron property of the substituent, the *meta*- and *para*-substituted isomers were more active than their *ortho*-substituted isomer with the Pt/MIL-101 catalyst. This might be explained in terms of steric hindrance of substituents. The Cl<sup>-</sup>, CH<sub>3</sub>– or CH<sub>3</sub>O– at the *ortho*-position of –NO<sub>2</sub> group with a comparatively larger size would bring stronger steric repulsion, so that attack of hydrogen to nitro group became more difficult under this circumstance.

As for selectivity to the hydrogenated product, it is almost over 99% except for those obtained with Cl<sup>-</sup>-substituted nitrobenzenes. By-products in these cases were phenyl amines derived from a side reaction of hydrodechlorination. Among all of the nitrobenzene derivatives, the 3-chloro-nitrobenzene was most active, furnishing a TOF of about  $25,500 \text{ h}^{-1}$ . Whereas the 2-methoxy-nitrobenzene was most inactive, only furnishing a TOF of  $77 \text{ h}^{-1}$  under the same conditions. It seemed that there was no obvious trend in electronic effect of substituted groups at different positions of phenyl ring in the catalytic performance of the Pt/MIL-101 catalysts, although the reason is still unclear at this moment.

**Table 3**

Hydrogenation of benzaldehyde with the Pt/MIL-101 catalyst in different solvents.

Entry	Solvent	Conv. (%) <sup>a</sup>
1	Water	59.4
2	Ethanol	61.1
3	Cyclohexane	44.1
4	Toluene	14.4

Reaction conditions: 50 mg 5 wt.% Pt/MIL-101 catalyst (0.06 mol% Pt), 21 mmol benzaldehyde, 20 mL solvent, 1200 rpm, 4.0 MPa H<sub>2</sub>, 1 h.

<sup>a</sup> Conversion was based on GC-FID.

### 3.3. Hydrogenation of benzaldehyde and its derivatives

Besides nitrobenzene and its derivatives, we also want to extend to liquid-phase hydrogenation of benzaldehyde and its derivatives with the Pt/MIL-101 and the Pt/35AS catalysts. We firstly screened solvent with the Pt/MIL-101 catalyst for hydrogenation of benzaldehyde in different solvents. As shown in Table 3, when the reaction was carried out in toluene, the hydrogenation of benzaldehyde only gave 14.4% conversion within 1 h (Table 3, entry 4). If cyclohexane was used as solvent, 44.1% conversion of benzaldehyde was achieved under the similar conditions (Table 3, entry 3). When the reaction was performed with the Pt/MIL-101 catalyst in water or in ethanol, comparable conversions (59.4–61.1%) were obtained (Table 3, entries 1 and 2). Therefore, water was applied as solvent for the follow-up studies.

Just like for the liquid-phase hydrogenation of nitrobenzene, the kinetic profile for the hydrogenation of benzaldehyde with the Pt/MIL-101 catalyst in water was investigated firstly. As shown in Fig. 6, at the beginning, only 14.6% conversion was obtained after 15 min. With reaction proceeding, the reaction was slightly accelerated. Conversions of benzaldehyde increased to 56.6% after 45 min and to 83.3% after 60 min. The reaction went slowly after 1 h. For the hydrogenation of benzaldehyde with the Pt/35AS catalyst, the kinetic profile demonstrated a nearly linear relationship between conversion and reaction time. About 31.0% conversion was obtained in the first 30 min and the reaction proceeded steadily, obtaining 59.0%, 78.0% and 92.0% conversions after 60 min, 90 min and 120 min, respectively.

Conversions obtained with both Pt catalysts are comparable for the hydrogenation of benzaldehyde in water, especially at the beginning. In order to equally compare catalytic performances of the two Pt catalysts, both Pt catalysts were applied to the hydrogenation of benzaldehyde derivatives in water. According to the

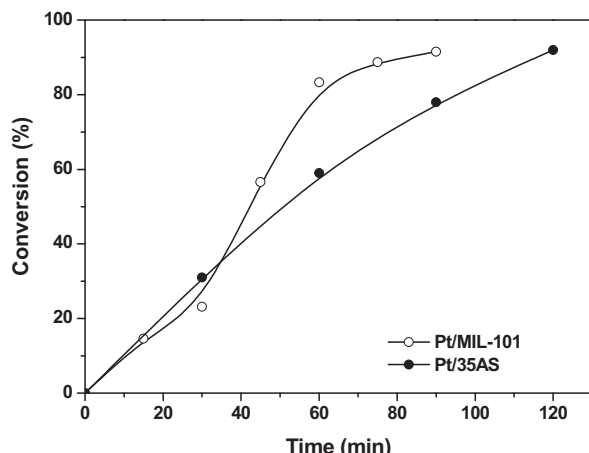


Fig. 6. Kinetic profile of benzaldehyde hydrogenation in water with the Pt/MIL-101 catalyst and the Pt/35AS catalyst. Reaction conditions: 21 mmol benzaldehyde, 4 MPa H<sub>2</sub>, 20 mL water, 298 K, 0.04 g Pt/MIL-101 catalyst (0.048 mol% Pt) or 0.05 g Pt/35AS catalyst (0.044 mol% Pt).

**Table 4**

Hydrogenation of benzaldehyde derivatives with different catalysts

		.
Entry	R-group	Catalyst
1	2-F	Pt/MIL-101
2		Pt/35AS
3	3-F	Pt/MIL-101
4		Pt/35AS
5	4-F	Pt/MIL-101
6		Pt/35AS
7	2-Cl	Pt/MIL-101
8		Pt/35AS
9	3-Cl	Pt/MIL-101
10		Pt/35AS
11	4-Cl	Pt/MIL-101
12		Pt/35AS
13	2-CH <sub>3</sub> O	Pt/MIL-101
14		Pt/35AS
15	3-CH <sub>3</sub> O	Pt/MIL-101
16		Pt/35AS
17	4-CH <sub>3</sub> O	Pt/MIL-101
18		Pt/35AS

Reaction conditions: 21 mmol substrate, 4 MPa H<sub>2</sub>, 20 mL water, 298 K, 0.04 g Pt/MIL-101 catalyst (0.048 mol% Pt), 1 h; 0.05 g Pt/35AS catalyst (0.044 mol% Pt), 1.5 h.

<sup>a</sup> Conversion was based on GC-FID.

kinetic profile of benzaldehyde hydrogenation on the Pt/MIL-101 catalyst, the hydrogenation of derivatives of benzaldehyde was conducted in 1 h. As listed in Table 4, for a strong electronegative substituent such as F-, conversions for the *ortho*-, *meta*- and *para*-fluorine substituted benzaldehydes were 97.6%, 96.4% and 88.2% with selectivities of 100% to the corresponding benzyl alcohol, respectively, (Table 4, entries 1, 3 and 5) with the Pt/MIL-101 catalyst. Among the F-substituted benzaldehydes, the *para*-substituted isomer was most inactive. While for a weak electronegative substituent Cl-, the *ortho*-Cl- substituted benzaldehyde was comparatively inactive, obtaining a conversion of 74.5%, lower than its *meta*- and *para*-substituted isomers, which afforded 87.5% and 85.3% conversions, respectively (Table 4, entries 7, 9 and 11). For an electron-donating group, such as methoxy, the *ortho*- and *meta*-substituted benzaldehydes obtained 94.1% and 80.1% conversions, respectively, much higher than that of their *para*-substituted isomer, only achieving 49.9% conversion under the same conditions (Table 4, entries 13, 15 and 17). Among all the substituted benzaldehydes, 2-fluoro-benzaldehyde afforded the highest activity, affording a 97.6% conversion within 1 h; while 4-methoxy-benzaldehyde showed the lowest activity, nearly a half of that for 2-fluoro-benzaldehyde.

Similar to those behaviors in the hydrogenation of nitroarenes, the Pt/35AS catalyst afforded lower conversions than the Pt/MIL-101 catalyst for the hydrogenation of benzaldehyde derivatives in most cases; even the reaction time was prolonged to 1.5 h for the Pt/35AS catalyst. For instance, for a strong electron-withdrawing substituent F-, the results were quite different from those obtained on the Pt/MIL-101 catalyst. The *meta*-substituted fluorobenzaldehyde was the most active isomer, obtaining a 98.2% conversion within 1.5 h, higher than the *ortho*- and *para*-substituted isomers, which afforded 64.4% and 72.5% conversions, respectively (Table 4, entries 2, 4 and 6). For another electron-withdrawing substituent Cl- group substituted benzaldehydes, all the three isomers gave comparable conversions (49.1–55.7%) (Table 4, entries 8, 10 and 12). For an electron-donating group methoxy-substituted benzaldehydes, the results were similar to those afforded by the Pt/MIL-101 catalyst. Both the *ortho*- and *meta*-substituted isomers achieved higher conversions (91.2–95.4%) than

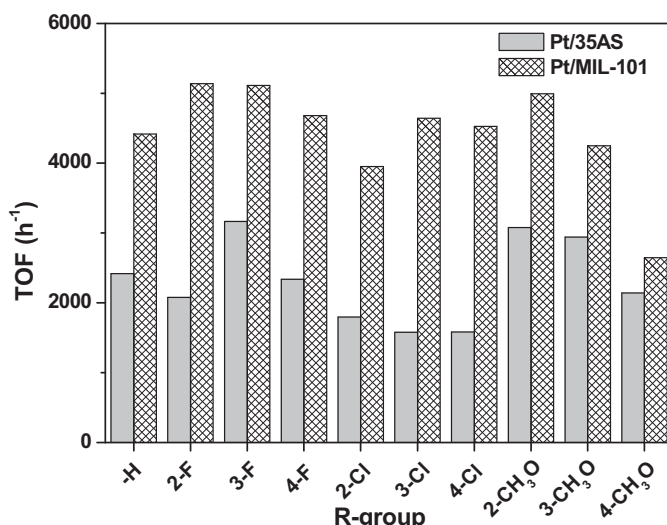


**Fig. 7.** Hydrogenation of benzaldehyde and its derivatives with the Pt/MIL-101 and Pt/35AS catalysts. The reaction conditions are identical to those in Table 4.

their *para*-substituted isomer, which only showed a conversion of 66.4% (Table 4, entries 14, 16 and 18). Just like nitrobenzenes series, the chlorine substituted benzaldehydes also afforded much lower selectivities to the corresponding benzyl alcohol and the by-product was benzyl alcohol, also originated from the hydrodechlorination side reaction. In addition, it seemed that there is no distinct trend in the steric effect for hydrogenation of benzaldehyde and its derivatives with two Pt catalysts as well.

Nevertheless, we noticed that even with the Pt/MIL-101 catalyst, hydrogenation of nitrobenzenes and benzaldehydes showed different trends in the case of methoxy-substituted isomers. This can be interpreted as follows: the *ortho*-methoxy-substituted nitrobenzene showed lower activity mainly due to larger steric hindrance of *ortho*-methoxy for  $-\text{NO}_2$  group. For methoxy-substituted benzaldehyde derivatives, both Pt/MIL-101 and Pt/35AS showed inferior activity for benzaldehyde derivative with methoxy group at the *para*-group. Although methoxy group at *ortho*- or *para*-position has similar conjugated effect, the methoxy group at *ortho*-position of aldehyde group would produce stronger inductive effect than the one at *para*-position, so that *ortho*-methoxy substituted benzaldehyde was more active than the *para*-substituted isomer.

In order to compare intrinsic activity of Pt catalysts supported on different materials in hydrogenation of benzaldehyde derivatives, the TOF values calculated as converted benzaldehydes per mol of exposed Pt atoms per hour according to the Pt loadings detected by ICP-AES were compared. As shown in Fig. 7, the Pt/35AS catalyst afforded the TOF values in the range of 1580–3165 h<sup>-1</sup>, varying with different substituent at phenyl ring. While for the Pt/MIL-101 catalyst, the TOF values varied from 2647 h<sup>-1</sup> to 5146 h<sup>-1</sup> with different substituents. Obviously, the Pt/MIL-101 catalyst afforded much higher activity than the Pt/35AS catalyst. The highest TOF of 5146 h<sup>-1</sup> was afforded by 2-fluoro-benzaldehyde with the Pt/MIL-101 catalyst. It is worth noting that these results are comparable with, in some cases even higher than, those obtained in our previous studies with Pt catalysts supported on other materials, such as periodic mesoporous resols (FDU-14), ordered mesoporous carbons (CMK-3 and CMK-8) and mesoporous composites ( $\text{TiO}_2@\text{SBA-15}$ ) [5–7].

#### 3.4. Reusability of the Pt/MIL-101 catalyst

Based on the discussions mentioned above, the Pt/MIL-101 catalyst was proved to be more active than the Pt/35AS catalyst for the

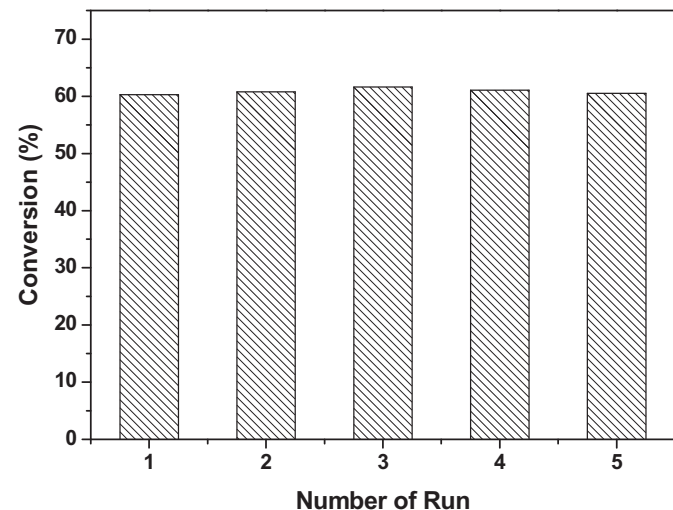


**Fig. 8.** Reusability of the Pt/MIL-101 catalyst toward the hydrogenation of benzaldehyde in ethanol. Reaction conditions: 0.04 g Pt/MIL-101 catalyst (0.048 mol% Pt), 21 mmol benzaldehyde, 20 mL ethanol, 4 MPa H<sub>2</sub> and 298 K, 1 h.

liquid-phase hydrogenation of benzaldehydes and nitrobenzenes. Nevertheless, reusability of the Pt/MIL-101 catalyst for liquid-phase hydrogenation of nitrobenzenes or benzaldehydes is also important to consider. Therefore, we performed recycling experiments of the Pt/MIL-101 catalyst for the liquid-phase hydrogenation of benzaldehyde. Considering that benzaldehyde and its hydrogenated product had a limited solubility in water compared with in ethanol, the recycling experiments were conducted in ethanol for convenient separation of benzaldehyde and its hydrogenated product from the Pt/MIL-101 catalyst after each cycle. As shown in Fig. 8, the Pt/MIL-101 catalyst could be used for at least five cycles without loss in activity. About 99% selectivity to benzyl alcohol was also kept constant during the recycling. The used Pt/MIL-101 catalyst was further characterized by ICP-AES to detect the Pt loading after five reaction cycles. As a result, the Pt loading was still 4.9 wt.% for the used Pt/MIL-101 catalyst. Compared with the fresh one, the Pt loading on the MIL-101 support was unchanged, indicating that the Pt nanoparticles were stable enough on the MIL-101 support.

#### 3.5. Discussion

The Pt/MIL-101 catalyst was much more active than the Pt/35AS catalyst in liquid-phase hydrogenation of nitrobenzene series and

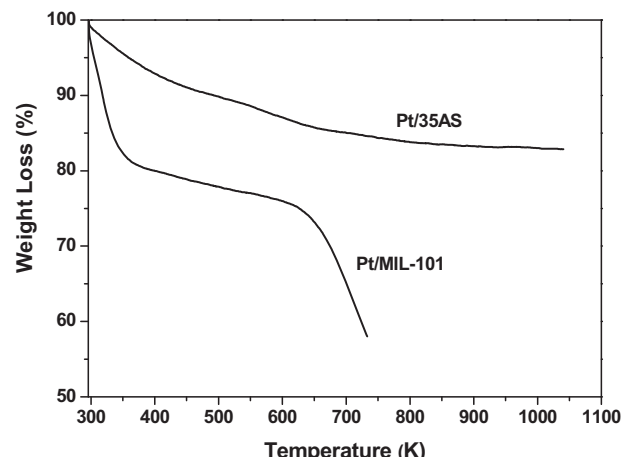


**Fig. 9.** TG curves of Pt/MIL-101 and Pt/35AS catalysts.

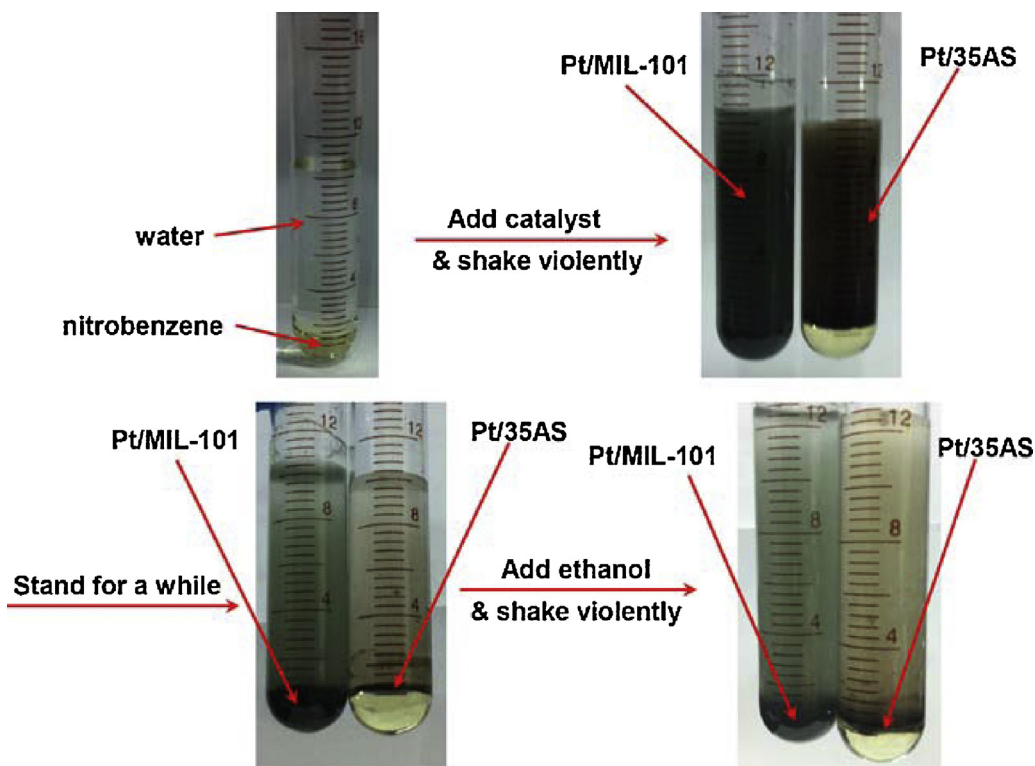


**Fig. 10.** The soakage properties of the Pt/MIL-101 and Pt/35AS catalysts.

benzaldehyde series and could be reused for several cycles. Based on characterization results, both Pt catalysts had an average Pt particle size of 2.4–2.9 nm with high dispersions. Thus, the two supported Pt catalysts can provide sufficient exposed Pt atoms to participate in hydrogenation reaction, especially for the Pt/35AS catalyst. Nevertheless, the Pt/MIL-101 catalyst gave higher activities than the Pt/35AS catalyst. We can deduce that the Pt particle size cannot be the determining parameter for two Pt catalysts with different performances; however, the support effect cannot be neglected. On the one hand, the MIL-101 MOFs had much larger specific surface area compared with the 35AS composites. On the other hand, MIL-101 and 35AS composites had different compositions: the former was constructed by the link of terephthalic acid and the vertex of chromium oxo trime; while the latter was composed of alumina and silica essentially. As well known, the different compositions would result in different surface properties in turn. In order to understand surface hydrophilicity & hydrophobicity of these materials, TG analysis was conducted under nitrogen atmosphere. As shown in Fig. 9, TG curves showed that weight loss of MIL-101 was mainly from physisorbed water because most of the weight loss took place below 373 K. The weight loss of MIL-101 at above 600 K was originated from decomposition of MIL-101. For the 35AS, weight loss was derived from desorption of chemisorbed water, as the weight loss was continuing till much higher temperature. This indicates that MIL-101 was more hydrophobic than 35AS.

Detailed soakage properties of these two catalysts can also be revealed from photographs displayed in Fig. 10. Because nitrobenzene is not soluble in water, nitrobenzene and water are kept in two phases, thus nitrobenzene is at the bottom and water is in the up phase. After Pt/MIL-101 and Pt/35AS catalysts were added separately and shaken violently, the Pt/MIL-101 catalyst was dispersed around the mixture; while the Pt/35AS catalyst was only dispersed in the aqueous phase. After the tubes were stood for a while, the

differences were obvious. The Pt/MIL-101 catalyst was dispersed in oil phase, while the Pt/35AS catalyst was located at the interface of water–oil due to gravitational settling. Although additional ethanol was added to these two tubes and shaken violently, the dispersion of these two catalysts did not change at all. Thus, either nitrobenzenes or benzaldehydes could be easily aggregated around the Pt/MIL-101 nanoparticles when reaction was performed in water, so that substrate concentration in water would be enriched around the Pt/MIL-101 catalyst, giving rise to a fast reaction compared with that with the Pt/35AS catalyst [5].

#### 4. Conclusion

Both the Pt/MIL-101 and Pt/35AS catalysts were active in the liquid-phase hydrogenation of nitroarenes and benzaldehyde and their derivatives. Nevertheless, the Pt/MIL-101 was much more active than the Pt/35AS catalyst under the same conditions mainly due to the more hydrophobic properties of MIL-101. For the hydrogenation of nitroarenes on Pt/MIL-101 catalyst in ethanol, up to  $25,438 \text{ h}^{-1}$  TOF was achieved. With respect to benzaldehyde and its derivatives, the TOF reached  $5146 \text{ h}^{-1}$  for 2-fluoro-benzaldehyde with the Pt/MIL-101 catalyst in water. Besides, the Pt/MIL-101 catalyst can be reused for at least four times without loss in activity or selectivity for the hydrogenation of benzaldehyde in ethanol.

#### Acknowledgements

This work was supported by the National Natural Science Foundation of China (NSFC grant nos. 21273076 and 21373089), the Open Research Fund of Top Key Discipline of Chemistry in Zhejiang Provincial Colleges and Key Laboratory of the Ministry of Education for Catalysis Materials (Zhejiang Normal University) (ZJHX2013), Programs Foundation of Ministry of Education (2012007613000), and Shanghai Leading Academic Discipline Project(B409).

## References

- [1] G. Brieger, T.J. Nestruck, *Chem. Rev.* 74 (1974) 567.
- [2] S. Sawadjooon, A. Lundstedt, J.S.M. Samec, *ACS Catal.* 3 (2013) 635.
- [3] P. Panagiotopoulou, D.G. Vlachos, *Appl. Catal. A* 480 (2014) 17.
- [4] L. Song, X. Li, H. Wang, H. Wu, P. Wu, *Catal. Lett.* 133 (2009) 63.
- [5] X. Li, Y. Shen, L. Song, H. Wang, H. Wu, Y. Liu, P. Wu, *Chem. Asian J.* 4 (2009) 699.
- [6] X. Li, W. Zheng, H. Pan, Y. Yu, L. Chen, P. Wu, *J. Catal.* 300 (2013) 9.
- [7] Y. Ding, X. Li, B. Li, H. Wang, P. Wu, *Catal. Commun.* 28 (2012) 147.
- [8] W. Du, G. Chen, R. Nie, Y. Li, Z. Hou, *Catal. Commun.* 41 (2013) 56.
- [9] Y. Liu, Y. Lu, M. Prashad, O. Repic, T. Blacklock, *Adv. Synth. Catal.* 347 (2005) 217.
- [10] R. Mantha, K. Taylor, N. Biswas, J. Bewtra, *Environ. Sci. Technol.* 35 (2001) 3231.
- [11] L. Bell, J. Devlin, R. Gillham, P. Binning, J. Contam. Hydrol. 66 (2013) 201–207.
- [12] Z. Sun, Y. Zhao, Y. Xie, R. Tao, H. Zhang, C. Huang, Z. Liu, *Green Chem.* 12 (2010) 1007.
- [13] S. Kataoka, Y. Takeuchi, A. Harada, T. Takagi, Y. Takenaka, N. Fukaya, H. Yasuda, T. Ohmori, A. Endo, *Appl. Catal. A* 427–428 (2012) 119.
- [14] S.R. Batten, N.R. Champness, X. Chen, J. Garcia-Martinez, S. Kitagawa, L. Ohrstrom, M. O'Keeffe, M.P. Suh, J. Reedijk, *CrystEngComm* 14 (2012) 3001.
- [15] J.Y. Lee, O.K. Farha, J. Roberts, K.A. Scheidt, S.B.T. Nguyen, J.T. Hupp, *Chem. Soc. Rev.* 38 (2009) 1450.
- [16] A. Corma, H. Garcia, F.X. Llabrés i Xamena, *Chem. Rev.* 110 (2010) 4606.
- [17] A. Dhakshinamoorthy, H. Garcia, *Chem. Soc. Rev.* 41 (2012) 5262.
- [18] H.R. Moon, D.W. Lim, M.P. Suh, *Chem. Soc. Rev.* 42 (2013) 1807.
- [19] G. Ferey, C. Mellot-Draznieks, C. Serre, F. Millange, J. Dutour, S. Surble, I. Margiolaki, *Science* 309 (2005) 2040.
- [20] A. Henschel, K. Gedrich, R. Krahnert, S. Kaskel, *Chem. Commun.* 4192 (2008).
- [21] N.V. Maksimchuk, K.A. Kovalenko, V.P. Fedin, O.A. Kholdeeva, *Adv. Synth. Catal.* 352 (2010) 2943.
- [22] N.V. Maksimchuk, K.A. Kovalenko, V.P. Fedin, O.A. Kholdeeva, *Chem. Commun.* 48 (2012) 6812.
- [23] L.H. Wee, F. Bonino, C. Lamberti, S. Bordiga, J.A. Martens, *Green Chem.* 16 (2014) 1351.
- [24] H. Pan, X. Li, D. Zhang, Y. Guan, P. Wu, *J. Mol. Catal. A* 377 (2013) 108.
- [25] H. Liu, Y. Li, R. Luque, H. Jiang, *Adv. Synth. Catal.* 353 (2011) 3107.
- [26] D. Zhang, Y. Guan, E.J.M. Hensen, L. Chen, Y. Wang, *Catal. Commun.* 41 (2013) 47.
- [27] J. Hermannsdorfer, R. Kempe, *Chem. Eur. J.* 17 (2011) 8071.
- [28] J. Juan-Alcaniz, J. Ferrando-Soria, I. Luz, P. Serra-Crespo, E. Skupien, V.P. Santos, E. Pardo, F.X. Llabrés i Xamena, F. Kapteijn, J. Gascon, *J. Catal.* 307 (2013) 295.
- [29] Z. Sun, G. Li, L. Liu, H. Liu, *Catal. Commun.* 27 (2012) 200.
- [30] H. Liu, Y. Liu, Y. Li, Z. Tang, H. Jiang, *J. Phys. Chem. C* 114 (2010) 13362.
- [31] A. Ajaz, A. Karkamkar, Y.J. Choi, N. Tsumori, E. Rönnebro, T. Autrey, H. Shiota, Q. Xu, *J. Am. Chem. Soc.* 134 (2012) 13926.
- [32] H. Dai, J. Su, K. Wu, W. Luo, G. Cheng, *Int. J. Hydrogen Energy* 39 (2014) 4947.
- [33] X. Gu, Z. Lu, H. Jiang, T. Akita, Q. Xu, *J. Am. Chem. Soc.* 133 (2011) 11822.
- [34] Q. Zhu, J. Li, Q. Xu, *J. Am. Chem. Soc.* 135 (2013) 10210.
- [35] A. Ajaz, Q. Xu, *J. Phys. Chem. Lett.* 5 (2014) 1400.
- [36] B. Yuan, Y. Pan, Y. Li, B. Yin, H. Jiang, *Angew. Chem. Int. Ed.* 49 (2010) 4054.
- [37] H. Wang, X. Li, Y.M. Wang, P. Wu, *ChemCatChem* 2 (2010) 1303.
- [38] X. Li, H. Wang, H. Pan, Y.M. Wang, P. Wu, *Appl. Catal. A* 488 (2014) 48.